Crystal Structure of the V^V Dimer [$V_2O_2(\mu\text{-}O)(dmpp)_2(OCH_3)_2$] and Its Equilibrium with the V^V Trimer [$V_3O_3(\mu\text{-}O)_3(dmpp)_3(H_2O)$]($H_2O$)$_2$ in Methanol/Water Solutions

Fernando Avecilla,*[a] Carlos F. G. C. Geraldes,[b] Anjos L. Macedo,[c] and M. Margarida C. A. Castro*[b]

The behaviour of the cyclic trimeric V^V complex [$V_3O_3(\mu\text{-}O)_3(dmpp)_3(H_2O)$]($H_2O$)$_2$, V_3L_3, (L = Hdmpp = 3-hydroxy-1,2-dimethyl-4-pyridinone) was studied in methanol and methanol/water solutions by using ^{51}V and 1D- and 2D ^1H NMR spectroscopy. Red crystals, isolated from a highly concentrated methanol solution of the trimeric complex, were analysed by X-ray crystallography. The solid-state structure of the compound showed the presence of a new dinuclear V^V cluster and allowed for its formulation as a [$V_2O_2(\mu\text{-}O)$-($dmpp$)$_2$(OCH_3)$_2$] complex, $V_2Y_2L_2$ (Y = OCH_3). This complex crystallises in the monoclinic system: $P2_1/c$, $a = 8.4573(11)$ Å, $b = 15.034(2)$ Å and $c = 15.849(2)$ Å, $\beta = 105.300(2)°$, $V = 1943{,}7(4)$ Å^3, $Z = 2$, and $R_1(wR_2) = 0.0492(0.1706)$. The trimer V_3L_3 complex dissolved in a dry methanol solution fully decomposes, as shown by the ^{51}V NMR signals at –388, –450 and –551 ppm, which are assigned to a monomer complex [VO(OMe)(dmpp)$_2$] (VYL$_2$), the dimer $V_2Y_2L_2$ and the monomethyl ester of monovanadate, V_1Y (V_1 = monovanadate; Y = OCH_3), respectively. In methanol/water solutions, a new ^{51}V NMR signal appears at $\delta = –492$ ppm, which is assigned to the [VO$_2$(dmpp)(H$_2$O)$_2$] (VL) complex. When the percentage of water in the mixture increases, the relative intensities of the $V_2Y_2L_2$ and V_1Y signals decrease sharply, and a broad signal at –488 ppm appears, corresponding to the original V^V trimer complex, which is the only species present in 94 % water. A temperature-dependent ^1H NMR study of a CD$_3$OD solution of V_3L_3 confirmed the presence, at room temperature, of the dinuclear V_2L_2 complex and the VL$_2$ species. At temperatures below 0 °C down to –50 °C, the appearance of new signals reflects the presence of isomers for the $V_2Y_2L_2$ and VYL$_2$ species with different stabilities and symmetries. 2D ^1H homonuclear NMR exchange experiments (EXSY) allowed us to establish the isomeric equilibria that take place in solution, and indicates intramolecular exchange between the two ligands of the major isomer of VYL$_2$ and intermolecular exchange between the major and minor isomers of species of different nuclearity, $V_2Y_2L_2$ and VYL$_2$. However, no evidence was found for intermolecular exchange between the major isomers and between the minor isomers of species of different nuclearity or between isomers of species of the same nuclearity.

(© Wiley-VCH Verlag GmbH & Co. KGaA, 69451 Weinheim, Germany, 2006)

Introduction

Vanadium is an essential biological trace element of the utmost importance.[1,2] It is present in some biological systems in high concentrations, where it seems to have a relevant role, such as in the *Amanita muscaria* mushroom as the amavadin complex[3] and in some ascideas in the form of tunichromes.[4] Vanadium is the cofactor of some enzymes, like the vanadium-dependent haloperoxidases in algae and lichens[5] and the vanadium-nitrogenases in some bacteria.[6] It also interferes with the activity of certain enzymes, in particular those involved in phosphorylations,[7] where it acts as a phosphate analogue, and it is responsible for many physiological and metabolic effects observed in different organisms, where it is essential at low concentrations although toxic at concentrations higher than 1 mM.[8] Vanadium in biological systems mainly occurs as the anionic vanadate (V^V), which is isostructural to phosphate, or the cationic vanadyl (V^{IV}), depending on the redox properties of the medium.[8] The insulin-mimetic properties of inorganic vanadate and vanadyl,[9] as well as of some V^{IV} and V^V complexes,[10] have stimulated the search for a vanadium complex that can be used as an effective oral substitute for insulin. The well-recognised biological importance of vanadium has attracted much interest for its coordination and redox chemistry both in the V^{IV} and V^V oxidation states and both in the solid state and in solution. The interest extends to the modeling of the interaction of vanadium

[a] Departamento de Química Fundamental, Universidade da Coruña,
Campus de A Zapateira s/n, 15071, A Coruña, Spain
E-mail: avecil@udc.es
[b] Departamento de Bioquímica, Centro de Espectroscopia RMN e Centro de Neurociências e Biologia Celular, Faculdade de Ciências e Tecnologia, Universidade de Coimbra,
Apartado 3126, 3001-401 Coimbra, Portugal
E-mail: gcastro@ci.uc.pt
[c] REQUIMTE, C.Q.F.B., Departamento de Química, Faculdade de Ciências e Tecnologia, Universidade Nova de Lisboa,
2829-516 Caparica, Portugal

with living systems, with particular focus on the structural and functional biological activity of this element.

The aqueous chemistry of vanadium(V) is very complex. Hydrolysis, redox and oligomerization reactions can occur in solution, resulting in different species, depending on the pH, ionic strength and total vanadium concentration in the medium,[11] which together determine the coordination properties of vanadium(V). The structure and reactivity of vanadate in other solvents, in particular alcohols, have been largely studied.[12] Vanadium complexes with different geometries and coordination modes containing O and/or N and/or S as donor atoms in their structures[6b,11,13] have been useful model compounds to understand the coordination chemistry of vanadium in living systems. In particular, the solid-state structures of V^{IV} and V^V compounds with ligands from the class of pyrones and pyridinones (with one ketonic and one enolic group as donor atoms) have been determined by X-ray crystallography[14a,15] and EXAFS.[16] The speciation of these vanadium compounds in solution has been extensively studied by using potentiomety, UV/Vis, ^{51}V and ^{1}H NMR and EPR spectroscopy.[14a,16–18] Compound bis(maltolato)oxidovanadium(IV) [BMOV, VO(ma)$_2$, ma = maltolate] was the first example to be used as an insulin-mimetic complex,[14,19] and phase 1 clinical trials in humans have been completed on bis(ethylmaltolato)oxidovanadium(IV) (BEOV).[20] Several other oxovanadium(IV) complexes have also been reported to exhibit insulin-mimetic properties in vivo.[21] The compound bis(3-hydroxy-1,2-dimethyl-4-pyridinone)oxidovanadium(IV), VO(dmpp)$_2$ (see Scheme 1 for the structure of the ligand Hdmpp), as well as the ternary systems formed with low molecular mass components of blood serum have also been studied in aqueous solution under anaerobic and aerobic conditions.[17,18] At physiological pH, VO(dmpp)$_2$ showed low toxicity in erythrocyte suspensions[22] and promising in vitro insulin-like properties in fibroblast cell lines[23a] and in rat adipocytes.[23b]
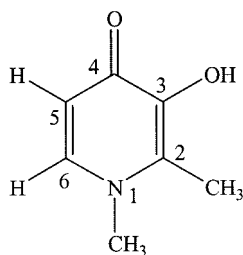
Scheme 1.

The interaction of vanadate with the ligand Hdmpp in aqueous solution has been extensively studied by us.[18] A new trinuclear oxovanadium(V) complex was isolated from aqueous solution at a pH of 4–5 and was characterised in the solid state by X-ray crystallography as [V$_3$O$_3$(μ-O)$_3$(dmpp)$_3$(H$_2$O)](H$_2$O)$_2$ that contains a cyclic V^V cluster and in aqueous solution by mass spectrometry and ^{51}V and ^{1}H NMR spectroscopy.[24] In this work, we report on the behaviour of this trinuclear V^V compound in methanol and

methanol/water solutions investigated by ^{51}V NMR spectroscopy and 1D and 2D ^{1}H NMR spectroscopy. The red crystals that formed from a highly concentrated CD$_3$OD solution of the V^V trimer were structurally analysed, and the X-ray crystallographic data obtained indicated the formation of a new dinuclear V^V compound [V$_2$O$_2$(μ-O)(dmpp)$_2$(OCH$_3$)$_2$].

Results and Discussion

X-ray Structure

The X-ray structure obtained for the crystalline [V$_2$O$_2$(μ-O)(dmpp)$_2$(OCH$_3$)$_2$] complex (V$_2$Y$_2$L$_2$) is shown in Figure 1 with the atomic numbering scheme, and the corresponding bond lengths and angles are listed in Table 1. It consists of a dinuclear oxovanadium(V) complex with two anionic dmpp ligands, one oxygen atom bridge and two methoxy groups, each coordinated to one vanadium atom. The oxygen atom bridge links the two vanadium atoms, each one of which is also coordinated to one oxo group. Both V1 and V2 atoms adopt a distorted six-coordinate octahedral geometry (Figure 2). The V1 coordination sphere is composed of an enolate oxygen atom [V1–O6 = 2.040(3) Å], a ketonic oxygen atom [V1–O7 = 1.989(3) Å], a deprotonated alkoxide oxygen atom of a methoxy group [V1–O1M = 1.787(4) Å], a terminal oxo atom [V1–O1 = 1.594(3) Å] and a second oxo atom [V1–O4 = 1.824(3) Å] that forms a strong bridge to V2 [V2–O4 = 1.804(3) Å]. The remainder of the V2 coordination sphere is completed by an enolate oxygen [V2–O3 = 2.060(3) Å], a ketonic oxygen atom [V2–O5 = 1.972(3) Å], an alkoxide oxygen atom of the other methoxy ligand [V2–O2M = 1.783(3) Å] and a terminal oxo atom [V2–O2 = 1.594(3) Å]. A second, weaker
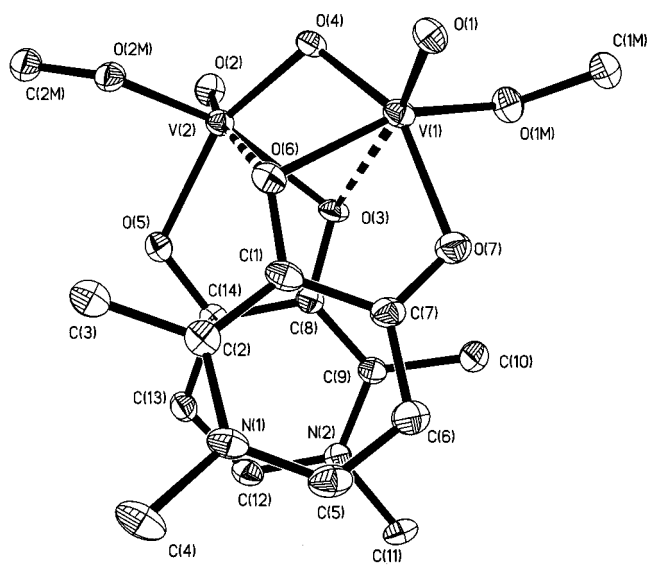

Figure 1. X-ray crystal structure of the complex [V$_2$O$_2$(μ-O)(dmpp)$_2$(OCH$_3$)$_2$] showing the atomic numbering scheme. Hydrogen atoms have been omitted for simplicity. The ORTEP plot is at the 30% probability level.

F. Avecilla, C. F. G. C. Geraldes, A. L. Macedo, M. M. C. A. Castro

bridge between V1 and V2 is formed by an enolate oxygen (O3) of the ligand coordinated to V2 (see Table 1) and an enolate oxygen (O6) of the ligand coordinated to V1. The V2–O3 and V1–O6 distances are 2.060(3) Å and 2.040(3) Å, respectively, as compared with the V1–O3 and V2–O6 bond lengths of 2.464(3) Å and 2.589(3) Å, respectively. The vanadium atom V1 is located at 0.33697 Å from the axial plane defined by O4, O6, O7 and O1M, and the vanadium atom V2 is 0.4010 Å from the basal plane defined by O3, O4, O5 and O2M (Figure 2). Both vanadium atoms have a strong V=O bond, as the values of the V1–O1 and V2–O2 distances are compatible with those found in other similar structures.[25] All bond lengths are in the range of the values

Table 1. Selected bond lengths [Å] and angles [°] for [V$_2$O$_2$(μ-O)(dmpp)$_2$(OCH$_3$)$_2$] with estimated standard deviations in parentheses. M indicates the methoxy oxygen atoms.

| Bond lengths			
V(1)–O(1)	1.594(3)	V(2)–O(2)	1.594(3)
V(1)–O(1M)	1.787(4)	V(2)–O(2M)	1.783(3)
V(1)–O(3)	2.464(3)	V(2)–O(3)	2.060(3)
V(1)–O(4)	1.824(3)	V(2)–O(4)	1.804(3)
V(1)–O(6)	2.040(3)	V(2)–O(5)	1.972(3)
V(1)–O(7)	1.989(3)	V(2)–O(6)	2.589(3)
Bond angles			
O(1)–V(1)–O(1M)	99.94(17)	O(2)–V(2)–O(2M)	101.51(17)
O(1)–V(1)–O(4)	104.13(17)	O(2)–V(2)–O(4)	104.61(17)
O(1M)–V(1)–O(4)	103.30(16)	O(2M)–V(2)–O(4)	102.85(15)
O(1)–V(1)–O(7)	101.56(17)	O(2)–V(2)–O(5)	100.86(17)
O(1M)–V(1)–O(7)	86.57(16)	O(2M)–V(2)–O(5)	87.46(15)
O(4)–V(1)–O(7)	150.29(15)	O(4)–V(2)–O(5)	149.83(15)
O(1)–V(1)–O(6)	99.11(16)	O(2)–V(2)–O(3)	101.90(16)
O(1M)–V(1)–O(6)	158.03(16)	O(2M)–V(2)–O(3)	154.64(15)
O(4)–V(1)–O(6)	82.46(14)	O(4)–V(2)–O(3)	80.46(14)
O(7)–V(1)–O(6)	78.95(14)	O(5)–V(2)–O(3)	78.69(13)
O(1)–V(1)–O(3)	171.68(16)	O(2)–V(2)–O(6)	171.03(15)
O(1M)–V(1)–O(3)	87.04(14)	O(2M)–V(2)–O(6)	85.82(14)
O(4)–V(1)–O(3)	69.59(12)	O(4)–V(2)–O(6)	68.37(12)
O(7)–V(1)–O(3)	83.25(13)	O(5)–V(2)–O(6)	84.49(13)
O(6)–V(1)–O(3)	74.99(12)	O(3)–V(2)–O(6)	71.85(12)
		V(2)–O(3)–V(1)	81.85(11)
		V(2)–O(4)–V(1)	110.33(16)
		V(1)–O(6)–V(2)	79.12(11)
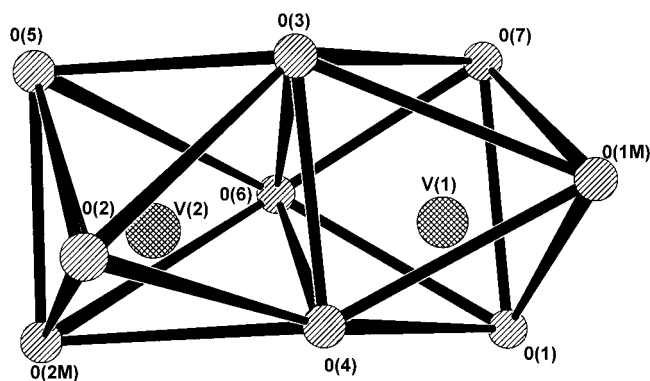
Figure 2. Coordination polyhedra in the crystal structure of the vanadium cluster in the dimeric species [V$_2$O$_2$(μ-O)(dmpp)$_2$(OCH$_3$)$_2$].

reported in the literature for other known polynuclear vanadium(V) complexes.[14a,15,26]

The oxido and methoxido ligands of the V$_2$Y$_2$L$_2$ dimer, which exert a strong *trans* influence, are *cis* to one another. The preference of these ligands for a *cis* configuration in such complexes has been demonstrated in VO(OMe)(L) compounds {where L represents the tetradentate Schiff bases *N,N'*-2,2-dimethyltrimethylenebis[salicylideniaminato(2–)] (salnptn) and *N,N'*-ethylenebis[salicylideneaminato(2–)] (salen)}.[27] In these complexes, a *cis*-VO(OMe) arrangement was allowed by forcing the normally planar tetradentate Schiff base ligands into three equatorial and one axial coordination positions. The oxido and methoxido ligands are also *cis* to one another in the *cis*-VO(OMe)-(ma)$_2$ complex, which results from aerobic oxidation of the bis(maltolato)oxidovanadium(IV) complex [VO(ma)$_2$, BOMV] in methanol.[14a,15a]

The V$_2$Y$_2$L$_2$ dimer complex has an enolic dmpp oxygen atom (O3 in V1) that is *trans* and four dmpp oxygen atoms (enolic O6 and ketonic O7 in V1, and enolic O3 and ketonic O5 in V2) that are *cis* relative to the strong V=O bond in each vanadium atom.[14a,15a] The dmpp oxygen atoms belonging to the enolic groups are deprotonated (O3 and O6). The *trans* position is destabilised with respect to the other positions, as shown by the length of the V1–O3 and V2–O6 bonds in the V$_2$Y$_2$L$_2$ species, in a manner similar to that in other dimeric and monomeric compounds.[28] The dmpp ligand has a strong preference for meridional coordination, except when a methoxy group or a water molecule competes with it for the *cis* position relative to the oxo group.

The dinuclear complex contains the V$_2$O$_3$ framework,[15b] which exhibits one bridging oxygen atom (O4) and the formal enolic oxygen atoms (O3 and O6) of the two dmpp groups. From the X-ray results one could not unambiguously distinguish between a keto-O5 and an enolate-O3 structure for this bifunctional binding group, as the C–O bond lengths to the formal keto and enolate oxygen atoms in the C–O–V–O–C chain are almost the same {e.g. C8–O3 [1.338(5) Å], C14–O5 [1.317(6) Å] for the V2 cycle}. It is possible that the π electron cloud is delocalised over all the atoms that form each C–O–V–O–C cycle, giving an intermediate character to all the formal ketonic and enolic oxygen atoms of each dmpp molecule.[24] As expected, the doubly bridging (O3 and O6) dmpp atoms have V–O bond [2.464(3) and 2.060(3) Å for (O3), 2.040(3) Å and 2.589(3) Å for (O6)] that are longer than the V–O bond for the bridging oxygen atom (O4) [1.824(3) and 1.804(3) Å]. The V2–O6 distance [2.589(3) Å] is even longer than the V1–O3 distance. The average value of the V–O–V bond lengths is 1.81(2), which is similar to that obtained for other polynuclear vanadium compounds.[29] In the V$_2$O$_3$ framework, the bond angle V1–O4–V2 [110.35(16)°] is very different from the bond angles V1–O3–V2 [81.81(11)°] and V1–O6–V2 [79.12(11)°]. This is in agreement with the results published for the trimeric species [V$_3$O$_3$(μ-O)$_3$(dmpp)$_3$(H$_2$O)](H$_2$O)$_2$.[24]

Figure 3 shows an upper view of the complex along the pseudo-C$_2$ axis, which passes along the oxygen atom O4.
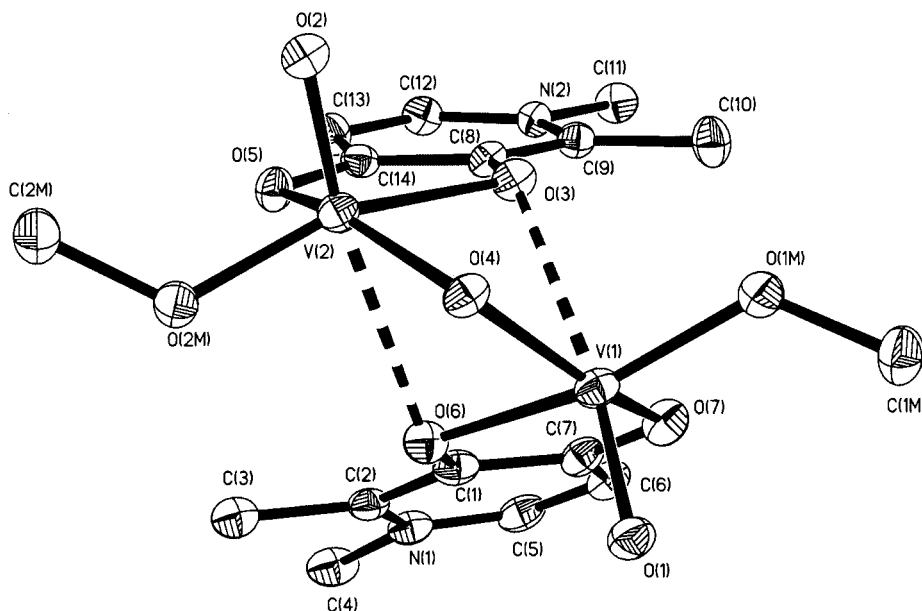
Figure 3. Upper view of the complex [V$_2$O$_2$(μ-O)(dmpp)$_2$(OCH$_3$)$_2$]. Hydrogen atoms have been omitted for simplicity. The ORTEP plot is at the 30% probability level.

This view clearly illustrates the pseudo-C_2 symmetry of the complex. Each of the two methoxy groups is coordinated to each of the two vanadium atoms. The angle between the planes of the two dmpp ligands is 34.6°. In this view, it is easy to foresee that a dynamic equilibrium between different isomers can occur in solution.

Solution Studies

^{51}V NMR Spectroscopic Studies

The behaviour of the cyclic V^V trimer compound [V$_3$O$_3$(μ-O)$_3$(dmpp)$_3$(H$_2$O)](H$_2$O)$_2$, (V$_3$L$_3$)[24] was studied as a function of solvent composition by ^{51}V NMR spectroscopy. Dissolution of black crystals of V$_3$L$_3$ in dry methanol gives a ^{51}V NMR spectrum that shows four signals with different intensities at –386 (shoulder), –388, –450 and –551 ppm (Figure 4A), which indicates the presence of four different vanadium(V) species in solution. The signal at –551 ppm corresponds to the monomethyl ester of vanadate V$_1$Y (V$_1$ = monovanadate; Y = OCH$_3$),[12c] which was previously detected as one of the products resulting from the aerobic oxidation in methanol solution of VO(ma)$_2$ to [VO(OCH$_3$)(ma)$_2$] and was described as [VO(OCH$_3$)]$^{2+}$.[15a] The signal at –450 ppm, with the highest intensity, was assigned to the dimer V^V complex V$_2$Y$_2$L$_2$. This assignment is corroborated by the observation of ^{51}V high frequency shifts of the signals for the dimer with respect to those of the monomer in other systems, such as the oxovanadium alkoxides VO(OR)$_3$ or vanadate complexes of hydroxy acids such as glycerate or lactate.[30]

In a highly concentrated methanol solution, this compound precipitates as red crystals, which were analysed by X-ray crystallography. The crystal structure is presented in this work. The signal at –388 ppm was assigned to *cis*-[VO(OCH$_3$)(dmpp)$_2$] (VYL$_2$) containing one methoxy
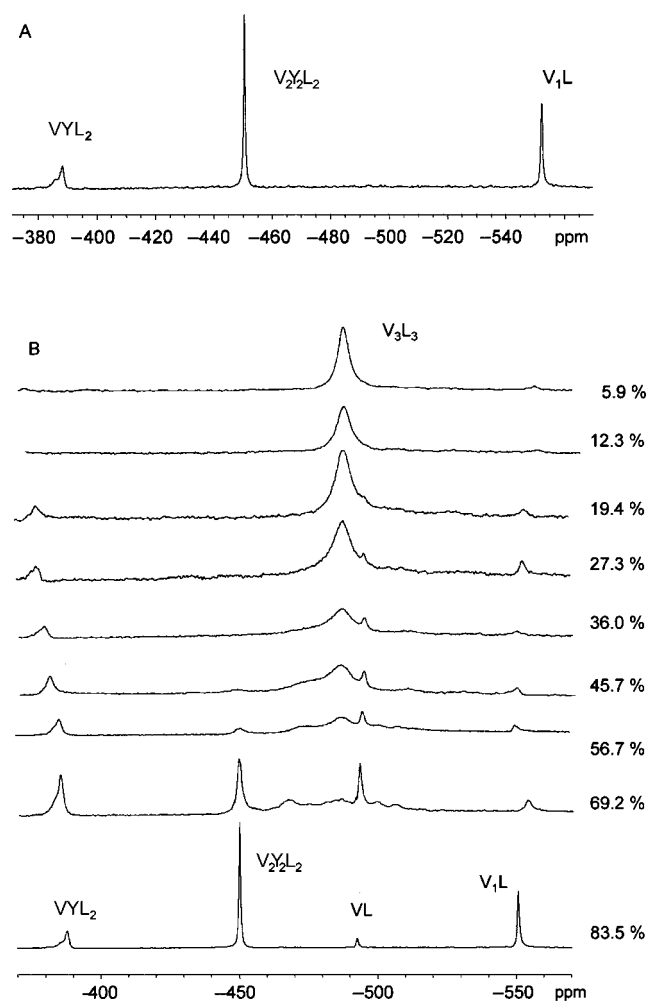

Figure 4. ^{51}V NMR spectra of solutions of the crystalline V^V compound [V$_3$O$_6$(dmpp)$_3$(H$_2$O)]·(H$_2$O)$_2$ obtained at 131.404 MHz and at 22.0±0.5 °C in (A) dry CH$_3$OH; (B) CH$_3$OH/H$_2$O mixtures, at pH ≈ 4 and different CH$_3$OH/H$_2$O mol ratios. The CH$_3$OH mol% is shown in the figure.

F. Avecilla, C. F. G. C. Geraldes, A. L. Macedo, M. M. C. A. Castro

group, analogous to the bis(maltolato) complex [VO(OCH$_3$)(ma)$_2$],[14a,15a] and its shoulder at –386 ppm to the corresponding *trans* isomer.

The ^{51}V NMR spectra of the trimer V$_3$L$_3$ dissolved in methanol/water solutions with different percentages of the two solvents dramatically change with the solvent composition, as shown in Figure 4B. In a solution where the mol fraction of CH$_3$OH is 83.5%, a new signal appears at δ = –492 ppm, in addition to those already present. This signal, which is absent in pure methanol and only appears when water is present in solution, was assigned to the [VO$_2$(dmpp)(H$_2$O)$_2$] (VL) complex with no methoxy group in its structure, which, at pH $\approx$ 4 appears at –492 ppm, as previously reported.[18] The relative intensities of the V$_2$Y$_2$L$_2$ and V$_1$Y signals decrease sharply when the percentage of water in the solution increases. The first signal completely disappears at 36.0% CH$_3$OH and the second one at 12.3% CH$_3$OH. The signals for the VL and VYL$_2$ species disappear at 12.3% CH$_3$OH. Furthermore, the VYL$_2$ signals gradually shift with increasing water content, up to a value of –376 ppm, reflecting the formation of the [VO(OH)(dmpp)$_2$] complex, which dominates in water solution at pH $\approx$ 4.[18] In addition, at 69.2% CH$_3$OH, a broad signal appears at –488 ppm. Its intensity increases with the percentage of water, and when water is present at 94.1%, it is the only signal observed in the ^{51}V NMR spectrum (Figure 4B). This signal corresponds to the original V^V trimer complex V$_3$L$_3$, whose ^{51}V NMR signal in aqueous solution at pH $\approx$ 4 has already been reported.[24] This was confirmed by slowly evaporating the methanol from a water/methanol solution of the V^V trimer at room temperature, which leads to an aqueous solution that gives a ^{51}V NMR spectrum consisting of the same single, broad signal at –488 ppm. After some time, black crystals were isolated from the solution, and characterisation of their structure by X-ray crystallography confirmed that these are indeed crystals of the V^V trimer V$_3$L$_3$ compound, whose structure had been previously reported.[24]

^{1}H NMR Spectroscopic Studies

^{1}H NMR spectra of solutions of the V^V trimer, [V$_3$O$_3$(μ-O)$_3$(dmpp)$_3$(H$_2$O)](H$_2$O)$_2$, in dry [D$_4$]MeOH (CD$_3$OD, no water present) were obtained at different temperatures. Figure 5A shows the signals for the H^5 and H^6 aromatic dmpp protons (6.0–8.0 ppm) from 25 °C down to –40 °C, while Figure 5B shows the signals corresponding to the H^5 (6.0–7.0 ppm) and C(2)–CH$_3$ (1.5–3.0 ppm) dmpp protons at –50 °C.[14,19] At 25 °C (Figure 5A) two doublets are observed at δ = 7.69 ppm and 7.55 ppm, corresponding to the H^6 protons of the V$_2$Y$_2$L$_2$ and VYL$_2$ species, respectively, and a doublet at δ = 6.55 ppm and a broad signal at δ = 6.28 ppm, assigned to the H^5 protons of the V$_2$Y$_2$L$_2$ and VYL$_2$ species, respectively. These assignments were made taking into account the ^{51}V NMR spectra previously discussed, which show the absence of the VYL and VL species when no water is present.
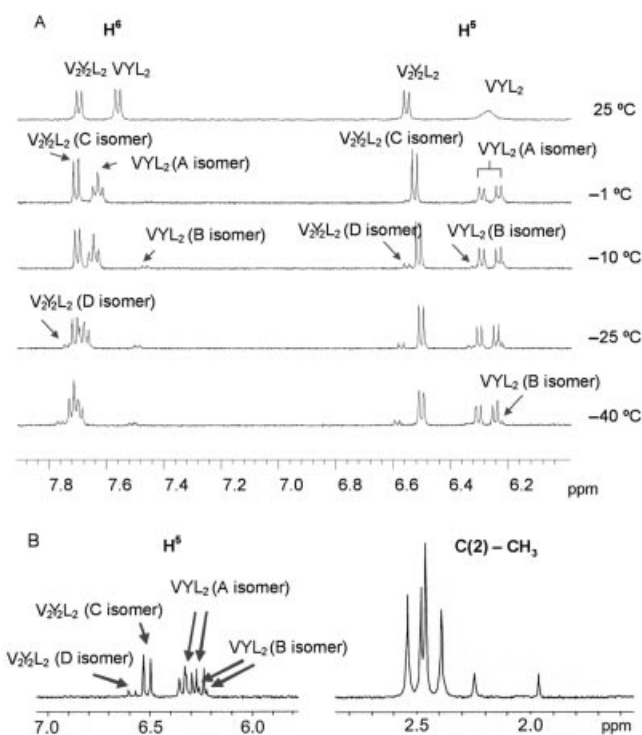

Figure 5. (A) 400 MHz ^{1}H NMR spectra of solutions of the crystalline V^V compound [V$_3$O$_6$(dmpp)$_3$(H$_2$O)]·(H$_2$O)$_2$ in CD$_3$OD, at different temperatures, showing only the signals corresponding to the H^5 and H^6 protons of the ligand dmpp; (B) 200 MHz ^{1}H NMR spectrum of a solution of the crystalline V^V compound [V$_3$O$_6$(dmpp)$_3$(H$_2$O)]·(H$_2$O)$_2$ in CD$_3$OD, at –50 °C, showing only the signals corresponding to the H^5 (6–7 ppm) and C(2)–CH$_3$ (1.5–3 ppm) protons of the ligand dmpp. The assignments in the spectra of Figure 5A are made according to the structures of the isomers presented in Figure 6.

The ^{1}H NMR spectra at lower temperatures become more complex, revealing the presence of isomers of these complexes in solution. At –1 °C, the 6.28 ppm (25 °C) broad signal splits into two doublets at δ = 6.32 ppm and 6.25 ppm, while the 7.55 ppm (25 °C) signal originates from the triplet centred at δ = 7.63 ppm formed by two partially overlapping doublets (Figure 5A, b), which correspond to the nonequivalent H^5 and H^6 protons of the two ligands of the VYL$_2$ compound.[14a,14c,19] These features reflect the slowing down of the intramolecular dynamic processes, which, at higher temperature, average the two different environments of the H^5 and H^6 protons of the two ligands in the dominant *cis* isomer of VYL$_2$ compound (isomer A, Figure 6A), making them nonequivalent. At –10 °C, the new low-intensity doublets appearing at δ = 6.32 ppm and δ = 7.45 ppm (Figure 5A) are indicative of the presence of isomeric forms, and correspond to the H^5 and H^6 protons of the less stable *trans* isomer of the VYL$_2$ species (isomer B, Figure 6B), respectively. The doublet at δ = 6.56 ppm with a weak intensity corresponds to the H^5 proton of an isomer of the V$_2$Y$_2$L$_2$ dimer with the methoxy groups in a *cis* position (Figure 6D); this isomer is less stable than the major isomer with *trans* methoxy groups (Figure 6C), which is similar to the structure obtained in the crystal form. This
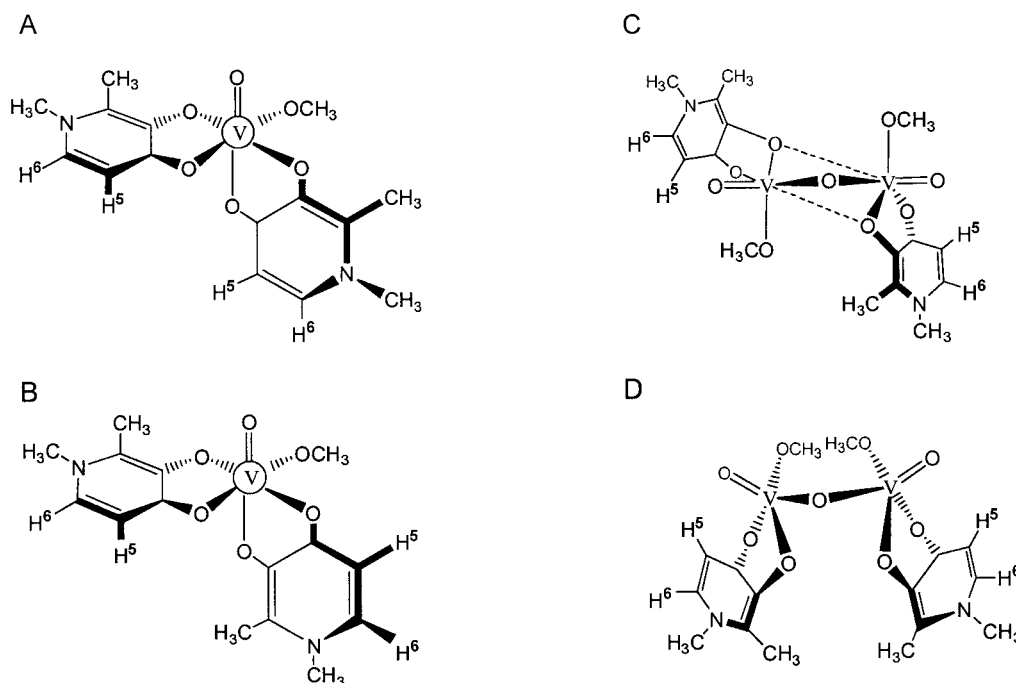
Figure 6. Schematic representation of the chemical structures of the possible isomers of: (A) the more stable and (B) the less stable isomers of the VYL$_2$ species [VO(dmpp)$_2$(OMe)]; and (C) the more stable and (D) the less stable isomers of the V$_2$Y$_2$L$_2$ species [V$_2$O$_2$(μ-O)-(dmpp)$_2$(OCH$_3$)$_2$], in methanol solution.

doublet is shifted to 6.57 ppm at –25 °C and to 6.58 ppm at –40 °C (Figure 5A). At –10 °C the H^6 signal of this isomer is not observed, as it overlaps with the large H^6 signal of the major V$_2$Y$_2$L isomer. However, at –25 °C it can be seen at δ = 7.75 ppm and it shifts to 7.76 ppm at –40 °C. At lower temperatures the signals of the H^6 proton of the two isomers of VYL$_2$ are shifted to higher frequencies– the signal of the major isomer (isomer A) becomes superimposed with the H^6 proton signals of the V$_2$Y$_2$L$_2$ compound.

A schematic representation of the proposed chemical structures of the two isomers for each of these two species, which is in agreement with the NMR spectroscopic data, is presented in Figure 6. From the ^{1}H NMR spectroscopic data, it is expected that the two H^6 protons of the dmpp ligands in the V$_2$Y$_2$L$_2$ compound are equivalent in each isomer; the same can be said for the two H^5 protons (Figure 6C and D). These protons in the VYL$_2$ species are nonequivalent in both isomers (Figure 6A and B), although they are indistinguishable at 25 °C (Figure 5A) because of the presence of intramolecular averaging processes that are fast on the NMR time-scale. The structures A and C of Figure 6 are assumed to represent the more stable isomers of VYL$_2$ and V$_2$Y$_2$L$_2$, respectively. This assumption is based on the present X-ray crystal structure data for V$_2$L$_2$ and on the literature data for VYL$_2$ (L = ma).[14,15] However, a more precise knowledge of the relative stability of the structures in solution would require a study involving theoretical energy calculations.

Figure 5B presents an ^{1}H NMR spectrum obtained at –50 °C that shows the spectral regions 5.8–7.0 ppm, corresponding to the H^5 protons, and 1.5–3.0 ppm, corresponding to the protons of the CH$_3$ group attached to the C(2) atom of the dmpp molecule. The different doublets corresponding to the H^5 protons in the different species in solution are better resolved and corroborate the presence of two isomers for the V$_2$Y$_2$L$_2$ complex (one doublet at δ = 6.51 ppm for the more stable isomer C and one doublet at δ = 6.59 ppm for the less stable isomer D) and two isomers of the VYL$_2$ compound (two doublets at δ = 6.24 ppm and 6.35 ppm for the less stable isomer B and two doublets at δ = 6.25 ppm and 6.31 ppm for the more stable isomer A). With respect to the protons of the C(2)–CH$_3$ group, six singlets are observed: two signals are assigned to the CH$_3$ protons of the two isomers of the V$_2$Y$_2$L$_2$ complex, each one corresponding to the six protons of the two equivalent CH$_3$ groups of each isomer, and the other four signals correspond to the four CH$_3$ groups (two nonequivalent CH$_3$ groups in each isomer of the VYL$_2$ complex).

2D NMR Spectroscopic Experiments

Two-dimensional (2D) ^{1}H NMR experiments, COSY (J correlated spectroscopy) and EXSY [exchange correlated spectroscopy, obtained using a phase-sensitive nuclear Overhauser spectroscopy (NOESY) pulse sequence], were carried out to further investigate the existence of different isomeric forms in solution, complementing the data obtained through one-dimensional (1D) ^{1}H NMR spectra at low temperature (–1 °C to –50 °C).

Figure 7 shows the low field region (6.0–8.0 ppm) of the 2D-COSY (Figure 7A) and 2D-EXSY (Figure 7B) spectra at –10 °C. This temperature value and the region in which the H^5 and H^6 signals of the dmpp ligand appear proved to
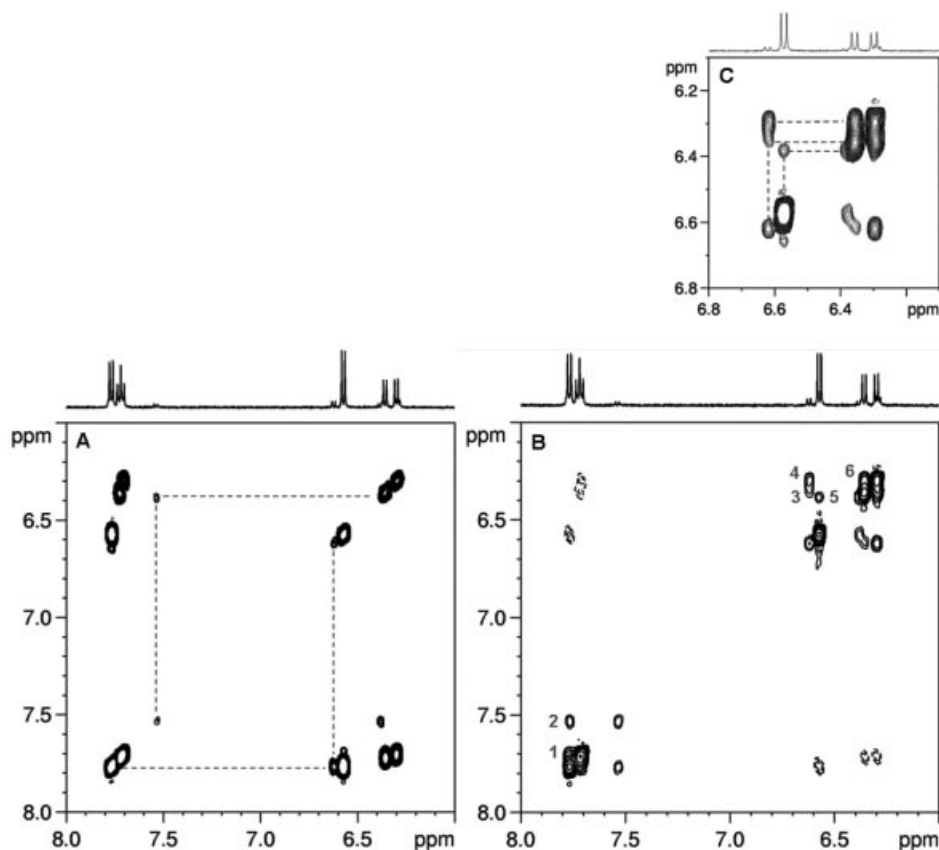
Figure 7. 400 MHz 2D ^{1}H homonuclear NMR spectra (spectral region 6–8 ppm) of solutions containing the V^V compound [V$_3$O$_6$-(dmpp)$_3$(H$_2$O)]·(H$_2$O)$_2$, in CD$_3$OD, at –10 °C: (A) COSY spectrum; and (B) EXSY spectrum (mixing time 800 ms) with (C) an expansion of the H^5 proton region. The contours of positive and negative peaks are defined by continuous and dashed lines, respectively.

give the most relevant information. In the COSY spectrum, cross-peaks correlating the protons H^5 and H^6 of each species in solution are expected. One cross-peak for each of the isomers C and D of V$_2$Y$_2$L$_2$, two cross-peaks for the two ligands of the major isomer of VYL$_2$ (isomer A) and only one of the two expected for its minor isomer (isomer B) can be observed. These observations confirm the assignments described above for the 1D ^{1}H NMR spectra.

The phase sensitive 2D-EXSY spectrum in the pure double absorption mode contains two types of cross-peaks. For small molecules, like those studied here, the cross-peaks resulting from nuclear Overhauser effects (nOes) that are based on the intramolecular dipolar interactions of protons H^5 and H^6 of the same ligand, which are close in space, have negative intensities and appear at the same positions as the COSY cross-peaks. Only three nOe cross-peaks are observed, two for the major isomer (A) of VL$_2$ and one for the major isomer (C) of V$_2$Y$_2$L$_2$, as those for the minor isomers could not be detected. The diagonal peaks and the exchange cross-peaks resulting from the exchange processes that occur between different species and/or between the isomeric forms of a given species have positive intensities. The exchange cross-peaks observed for mixing times $\tau_m > 1/R$, where $R = k_{ex}/\Delta v_o$ is the ratio of the exchange rate constant and the chemical shift difference between the exchanging peaks of the same proton in the two species, give useful

information about the dynamic equilibria in solution.[31] Their intensities are related to the corresponding exchange rate constants of the exchange equilibrium. A qualitative analysis of the exchange patterns of Figure 7B shows six cross-peaks, two in the H^5 region and four in the H^6 region. In the H^5 region, there are two stronger correlations – one between the two ligands of the major isomer of VYL$_2$ (A) and one between the minor isomer of V$_2$Y$_2$L$_2$ (D) and one of the two H^5 protons of the major isomer of VYL$_2$ (A). Two weaker correlations in the H^5 region are observed between the minor isomer of V$_2$Y$_2$L$_2$ (D) and the other H^5 protons of the major isomer of VL$_2$ (A), and between the major isomer of V$_2$Y$_2$L$_2$ (C) and the minor isomer of VYL$_2$ (B). In the H^6 region, two weak cross-peaks are observed – one involving correlation of the major or minor isomers of V$_2$Y$_2$L$_2$ (C or D) with the major isomer of VYL$_2$ (A) and the other with its minor isomer (B). This uncertainty results from the overlap of the H^6 resonances of isomers C and D of V$_2$Y$_2$L$_2$. However, taking into account the exchange pattern observed for the H^5 protons, the A↔D and B↔C correlations between the H^6 protons are more plausible. There is no evidence of cross-peaks correlating the H^5 or H^6 protons of the two isomers of the same species.

In conclusion, the ^{51}V NMR spectroscopic data show that two different oligomeric species containing V^V and dmpp can be isolated in water and methanol. Their X-ray

crystal structures show that the water species is a cyclic V$_3$L$_3$ trimer, [V$_3$O$_3$(μ-O)$_3$(dmpp)$_3$(H$_2$O)](H$_2$O)$_2$, while the methanol species is a V$_2$Y$_2$L$_2$ dimer, [V$_2$O$_2$(μ-O)(dmpp)$_2$-(OCH$_3$)$_2$]. Dissolution of black crystals of the V$_3$L$_3$ trimer in methanol leads to its complete dissociation into a V$_2$Y$_2$L$_2$ dimer, a VYL$_2$ monomer and monovanadate, each of which has one methoxy group coordinated to the V^V atoms. Red crystals of the dimer were isolated from the methanol solution. Increasing the amount of water in mixtures with methanol leads successively to the appearance of VL, the disappearance of V$_2$Y$_2$L$_2$ and the monomer species, while the trimer dominates at high water content.

On the basis of the results from the 2D-EXSY NMR experiments, the following intermolecular exchange equilibria between the different species were detected in a CD$_3$OD solution of the trimer V^V complex:

V$_2$Y$_2$L$_2$ (C isomer) ⇆ VYL$_2$ (B isomer)

V$_2$Y$_2$L$_2$ (D isomer) ⇆ VYL$_2$ (A isomer)
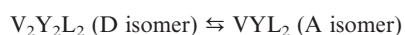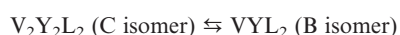
These equilibria involve exchange between the major isomer and the minor isomer of species of different nuclearity. Intramolecular exchange was also detected between the two ligands of VYL$_2$ (isomer A), but no evidence was found for intermolecular exchange between the major and minor isomers of species of different nuclearity or between isomers of species of the same nuclearity.

Experimental Section

Reagents: Sodium metavanadate, NaVO$_3$, and methanol were purchased from Sigma, and the ligand 1,2-dimethyl-3-hydroxy-4-pyridinone (Hdmpp) from ACROS Organics and used without further purification. KOH, HCl and CH$_3$OH were obtained from Merck, while KOD, DCl, D$_2$O (99.9 atom% D) and CD$_3$OD (99.9 atom% D) from Cambridge Isotope Laboratories. All the experiments were carried out under aerobic conditions.

Synthesis: The synthesis of the trimer [V$_3$O$_3$(μ-O)$_3$(dmpp)$_3$-(H$_2$O)](H$_2$O)$_2$ was carried out following the procedure described in the literature.[24] Red crystals of [V$_2$O$_2$(μ-O)(dmpp)$_2$(OCH$_3$)$_2$] were isolated from methanolic solution of the trimer; however, under atmospheric conditions these crystals turn black after replacement of methanol by water.

Solutions: Solutions of the trimer [V$_3$O$_3$(μ-O)$_3$(dmpp)$_3$(H$_2$O)]-(H$_2$O)$_2$ used for the ^{51}V NMR spectroscopic experiments contained CH$_3$OH or CH$_3$OH/H$_2$O mixtures, and were prepared by dissolving the appropriate amount of the solid compound in the solvent (or solvents) in order to have the desired concentrations. The CH$_3$OH/H$_2$O mol ratios were checked by integration of the ^{1}H NMR signals of the solvents. 1D ^{1}H NMR spectra as well as 2D ^{1}H COSY and EXSY NMR spectra were acquired in CD$_3$OD solutions. pH values were measured by using a Crison MicropH 2002 pH meter with an Ingold 405-M5 combined electrode.

Methods

NMR Spectroscopy: ^{51}V NMR spectra at 22.0 ± 0.5 °C were recorded with a Varian Unity-500 Spectrometer operating at 131.404 MHz, using a 5 mm broad band probe. ^{51}V NMR chemical shifts were externally referenced to a VOCl$_3$ solution at 0 ppm. The ^{51}V NMR acquisition parameters were: 33 kHz spectral width, 25 µs pulse width, 0.5 s acquisition time and 10 Hz line broadening.

^{1}H NMR spectra were obtained by using a pre-saturation pulse sequence to eliminate the residual water signal. The low-temperature 1D and the 2D ^{1}H NMR spectra were obtained with a Bruker ARX400 NMR Spectrometer operating at 400.13 MHz, using a 5 mm inverse probe and a controlled-temperature unit. Magnitude COSY and phase sensitive NOESY (800 ms mixing time) were acquired with a spectral width of 4000 Hz in both F1 and F2, with 1024×256 data points. Spectra were processed with unshifted sine bell (COSY) and sine^2 (NOESY) functions. The ^{1}H NMR spectrum at –50 °C was obtained with a Bruker AC 200 F Spectrometer operating at 200.13 MHz, using a 5-mm probe and a controlled-temperature unit.

ES Mass Spectrum: Electron spray (ES) mass spectra were recorded with an MSD spectrometer with a fragmentation of 50 V in a mixture of 98% methanol/2% formic acid: m/z = 457 [V$_2$O$_3$-(C$_7$H$_8$O$_2$N)$_2$(OCH$_3$)]$^+$, 343 [VO(C$_7$H$_8$O$_2$N)$_2$]$^+$, 236 [VO-(C$_7$H$_8$O$_2$N)(OCH$_3$)]$^+$.

X-ray Crystallography: The crystalline trimer [V$_3$O$_3$(μ-O)$_3$(dmpp)$_3$-(H$_2$O)](H$_2$O)$_2$ was dissolved in methanol until saturation was reached. After a few hours, slow evaporation of this solution gave dark red crystals of X-ray quality. A suitable crystal of [V$_2$O$_2$(μ-O)(dmpp)$_2$(OCH$_3$)$_2$] was coated with Fomblin oil, placed at the end of a silica fibre and mounted on a goniometer head of a Bruker SMART CCD diffractometer in a stream of cold nitrogen gas. These crystals are unstable and turn black when left in contact with atmospheric conditions.

Selected crystallographic data are shown in Table 2. Three-dimensional X-ray data were collected at low temperature (173 K) in the range 1.90 < 2θ < 28.32° with a Siemens SMART 1000 CCD diffractometer by the Ω-scan method. Complex scattering factors were taken from the programme package SHELXTL.[32] The structure was solved by direct methods and refined by using full-matrix least-squares methods on F^2. The data were processed and corrected for Lorentz and polarisation effects and for absorption (semi-empirical method). The non-hydrogen atoms were refined with anisotropic thermal parameters in all cases. The hydrogen atoms were refined to carbon, which were placed in idealised positions and refined by using a riding mode. A final difference Fourier map showed no residual density outside –1.064 to +0.845 e Å^{-3}. Selected bond lengths and bond angles appear in Table 1.

Table 2. Crystallographic data for the complex [V$_2$O$_2$(μ-O)-(dmpp)$_2$(OCH$_3$)$_2$].

Empirical formula	C$_{16}$H$_{22}$N$_2$O$_9$V$_2$
Formula mass [g mol^{-1}]	488.24
Crystal system	monoclinic
Space group	$P2_1/c$
a [Å]	8.4573(11)
b [Å]	15.034(2)
c [Å]	15.849(2)
$β$ [°]	105.300(2)
V [Å^3]	1943.7(4)
Z	2
T [K]	173(2)
$λ$ [Å]	0.71073
$D_{calcd.}$ [g·cm^{-3}]	1.668
F (000)	1000
No. of reflections collected	10939
No. of observed reflections	3038
R_1[a]	0.0492
wR_2 (all data)	0.1706
Largest diff peak and hole [e Å^{-3}]	0.845/–1.064

[a] $R_1 = \Sigma||F_o| - |F_c|| / \Sigma|F_o|$, $wR_2 = \{\Sigma[w(||F_o|^2 - |F_c|^2|)^2] / \Sigma[w(F_o^4)]\}^{1/2}$.

F. Avecilla, C. F. G. C. Geraldes, A. L. Macedo, M. M. C. A. Castro

CCDC-602237 contains the supplementary crystallographic data for this paper. These data can be obtained free of charge from The Cambridge Crystallographic Data Centre via www.ccdc.cam.ac.uk/data_request/cif.

Acknowledgments

[1] N. D. Chasteen (Ed.), *Vanadium in Biological Systems*, Kluwer, Dordrecht, The Netherlands, **1990**.

[2] H. Sigel, A. Sigel (Eds.), *Metal Ions in Biological Systems*, Marcel Dekker, Inc., New York, **1995**, vol. 31.

[3] E. M. Armstrong, R. L. Beddoes, L. J. Calviou, J. M. Charnock, D. Collison, N. Ertok, J. H. Naismith, C. D. Garner, *J. Am. Chem. Soc.* **1993**, *115*, 807–808.

[4] a) M. J. Smith, *Experiencia* **1989**, *45*, 452; b) S. W. Taylor, B. Kammerer, E. Bayer, *Chem. Rev.* **1997**, *97*, 333–346.

[5] H. Vilter, *Phytochemistry* **1984**, *23*, 1387–1390.

[6] a) R. L. Robson, R. R. Eady, T. H. Richardson, R. W. Miller, M. Hawkins, J. R. Postgate, *Nature (London)* **1986**, *322*, 388–390; b) D. Rehder, *Coord. Chem. Rev.* **1999**, *182*, 297–322; c) R. R. Eady, *Coord. Chem. Rev.* **2003**, *237*, 23–30.

[7] a) P. J. Stankiewicz, A. S. Tracey and D. C. Crans, "Vanadium and its Role in Life" in *Metal Ions in Biological Systems* (Eds.: H. Sigel, A. Sigel), Marcel Dekker, New York, **1995**, vol. 31, ch. 9; b) A. B. Goldfine, G. Willksy, C. R. Kahn in *Vanadium Compounds: Biochemistry Chemistry, and Therapeutic Applications* (Eds.: A. S. Tracey, D. C. Crans), American Chemical Society, Washington, DC, **1998**.

[8] N. D. Chasteen, "The Biochemistry of Vanadium" in *Structure and Bonding* **1983**, *53*, 105–138.

[9] a) Y. Shechter, S. J. D. Karlish, *Nature* **1980**, *284*, 556–558; b) H. Sakurai, K. Tsuchiya, M. Nukatsuka, M. Sofue, J. Kawada, *J. Endocrinol.* **1990**, *126*, 451–459; c) K. Kawabe, M. Tadokoro, Y. Kojima, Y. Fujisawa, H. Sakurai, *Chem. Lett.* **1998**, 9–10.

[10] a) D. C. Crans, L. Yang, J. A. Alfano, L.-H. Chi, W. Jin, M. Mahroof-Tahir, K. Robbins, M. M. Toloue, L. K. Chan, A. J. Plante, R. Z. Grayson, G. R. Willsky, *Coord. Chem. Rev.* **2003**, *237*, 13–22; b) H. Sakurai, H. Yasui, Y Adachi, *Expert Opin. Invest. Drugs* **2003**, *12*, 1189–1203.

[11] D. Rehder, *Angew. Chem. Int. Ed. Engl.* **1991**, *30*, 148–167.

[12] a) M. J. Gresser, A. S. Tracey, *J. Am. Chem. Soc.* **1986**, *108*, 1935–1939; b) A. S. Tracey, M. J. Gresser, *Can. J. Chem.* **1988**, *66*, 2570–2574; c) A. S. Tracey, M. J. Gresser, B. Galeffi, *Inorg. Chem.* **1988**, *27*, 157–161.

[13] D. C. Crans, J. J. Smee, E. Gaidamauskas, L. Yang, *Chem. Rev.* **2004**, *104*, 849–902.

[14] a) P. Caravan, L. Gelmini, N. Glover, F. G. Herring, H. Li, J. H. McNeill, S. J. Rettig, I. A. Setyawati, E. Shuter, Y. Sun, A. S. Tracey, V. G. Yuen, C. Orvig, *J. Am. Chem. Soc.* **1995**, *117*, 12759–12770; b) J. H. McNeil, V. G. Yuen, H. R. Hoveyda, C. Orvig, *J. Med. Chem.* **1992**, *35*, 1489–1491; c) G. R. Hanson, Y. Sun, C. Orvig, *Inorg. Chem.* **1996**, *35*, 6507–6512.

[15] a) Y. Sun, B. R. James, S. J. Rettig, C. Orvig, *Inorg. Chem.* **1996**, *35*, 1667–1673; b) Y. Sun, M. Melchior, D. A. Summers, R. C. Thompson, S. J. Rettig, C. Orvig, *Inorg. Chem.* **1998**, *37*, 3119–3121.

[16] J. Burgess, B. de Castro, C. Oliveira, M. Rangel, W. Schlindwein, *Polyhedron* **1997**, *16*, 789–794.

[17] a) M. M. C. A. Castro, C. F. G. C. Geraldes, P. Gameiro, E. Pereira, B. Castro, M. Rangel, *J. Inorg. Biochem.* **2000**, *80*, 177–179; b) M. Rangel, *Transition Met. Chem.* **2001**, *26*, 219–223.

[18] a) M. M. C. A. Castro, F. Avecilla, C. F. G. C. Geraldes, B. de Castro, M. Rangel, *Inorg. Chim. Acta* **2003**, *356*, 142–154; b) P. Buglyo, T. Kiss, E. Kiss, D. Sanna, E. Garriba, G. Micera, *J. Chem. Soc., Dalton Trans.* **2002**, 2275–2282.

[19] A. Katoh, K. Kazutoshi, R. Saito, Y. Fujisawa, T. Takino, H. Sakurai, *Heterocycles* **2003**, *60*, 1147–1159.

[20] K. H. Thompson, B. D. Liboiron, Y. Sun, K. D. D. Bellman, I. A. Setyawati, B. O. Patrick, V. Karunaratne, G. Rawji, J. Wheeler, K. Sutton, S. Bhanot, C. Cassidy, J. H. McNeill, V. G. Yuen, C. Orvig, *J. Biol. Inorg. Chem.* **2003**, *8*, 66–74.

[21] a) P. Poucheret, R. Gross, A. Cadene, M. Manteguetti, J. Serrano, G. Ribes, G. Cross, *Mol. Cell. Biochem.* **1995**, *153*, 197–204; b) H. Sakurai, K. Fujii, H. Watanabe, H. Tamura, *Biochem. Biophys. Res. Commun.* **1995**, *214*, 1095–1101; c) H. Sakurai, K. Tsuchiya, M. Nukatsuka, J. Kawada, S. Ischikawa, H. Yoshida, M. Komatsu, *J. Clin. Biochem. Nutr.* **1990**, *8*, 193–200; d) H. Watanabe, M. Nakai, K. Komazawa, H. Sakurai, *J. Med. Chem.* **1994**, *37*, 876–877; e) J. H. McNeill, V. G. Yuen, S. Dai, C. Orvig, *Mol. Cell. Biochem.* **1995**, *153*, 175–180; f) H. Sakurai, K. Fujii, S. Fujimoto, Y. Fujisawa, K. Takechi and H. Yasui in *ACS Symposium Series 711* (Ed.: A. S. Tracey and D. C. Crans), American Chemical Society, Washington D.C., **1998**, p. 344; g) H. Sakurai, Y. Fujisawa, S. Fujimoto, H. Yasui, T. Takino, *J. Trace Elem. Exp. Med.* **1999**, *12*, 393–401.

[22] T. C. Delgado, A. I. Tomaz, I. Correia, J. C. Pessoa, J. G. Jones, C. F. G. C. Geraldes, M. M. C. A. Castro, *J. Inorg. Biochem.* **2005**, *99*, 2328–2339.

[23] a) D. Rehder, J. C. Pessoa, C. F. G. C. Geraldes, M. M. C. A. Castro, T. Kabanos, T. Kiss, B. Maier, G. Micera, L. Petterson, M. Rangel, A. Salifoglou, I. Turel, D. Wang, *J. Biol. Inorg. Chem.* **2002**, *7*, 384–396; b) M. Rangel, A. Tamura, C. Fukushima, H. Sakurai, *J. Biol. Inorg. Chem.* **2001**, *6*, 128–132.

[24] F. Avecilla, C. F. G. C. Geraldes, M. M. C. A. Castro, *Eur. J. Inorg. Chem.* **2001**, 3135–3142.

[25] F. Jiang, P. A. Oren, S. M. Miller, J. Chen, M. Mahroof-Tahir, D. C. Crans, *Inorg. Chem.* **1998**, *37*, 5439–5451.

[26] a) K. Isobe, S. I. Ooi, Y. Nakamura, S. Kawaguchi, H. Kuroya, *Chem. Lett.* **1975**, 35–38; b) C. R. Cornman, J. Kampf, M. S. Lah, V. L. Pecoraro, *Inorg. Chem.* **1992**, *31*, 2035–2043; c) X. Li, M. S. Lah, V. L. Pecoraro, *Inorg. Chem.* **1988**, *27*, 4657–4664.

[27] S. A. Fairhust, D. L. Hughes, U. Kleinkes, J. G. Leigh, J. R. Sanders, J. Weisner, *J. Chem. Soc., Dalton Trans.* **1995**, 321–326.

[28] C. J. Carrano, C. M. Nunn, R. Quan, J. A. Bonadies, V. L. Pecoraro, *Inorg. Chem.* **1990**, *29*, 944–951.

[29] a) I. Cavaco, J. Costa-Pessoa, M. T. Duarte, P. M. Matias, R. T. Henriques, *Polyhedron* **1993**, *12*, 1231–1237; b) W. Priebsch, D. Rehder, M. von Oeynhausen, *Chem. Ber.* **1991**, *124*, 761–764; c) H. Rieskamp, P. Gietz, R. Mattes, *Chem. Ber.* **1976**, *109*, 2090–2096.

[30] a) D. Paulsen, D. Rehder, D. Thoennes, *Z. Naturforsch., Teil A* **1978**, *33*, 834–839; b) D. Rehder, *Bull. Magn. Reson.* **1982**, *4*, 33–83; c) A. S. Tracey, M. Gresser, K. M. Parkinson, *Inorg. Chem.* **1987**, *26*, 629–638.

[31] a) G. Otting, E. Liepinsh, K. Wüthrich, *J. Am. Chem. Soc.* **1990**, *113*, 4363–4364; b) D. Neuhaus, M. Williamson (Eds.), "The Nuclear Overhauser Effect" in *Structural and Conformational Analysis*, 2nd ed., Wiley-VCH Inc., Chichester, United Kingdom, **2000**.

[32] G. M. Sheldrick, *SHELXTL Bruker Analytical X-ray System*, ver. 5.01, Madison, WI, **1997**.